Buckling of Laminated Anisotropic Imperfect Circular Cylinders under Axial Compression

R. C. TENNYSON*
University of Toronto, Toronto, Ontario, Canada

AND

D. B. MUGGERIDGE†
Fleet Manufacturing Ltd., Fort Erie, Ontario, Canada

A new design approach is presented to provide a conservative estimate of the buckling strength of laminated anisotropic circular cylinders under axial compression. The analysis is based on Koiter's "special theory" for uniform axisymmetric shape imperfections which is valid for imperfections of the order of the shell wall thickness. Fourteen three-ply, glass-epoxy cylinders containing random imperfections of small mean square amplitude were characterized in terms of an equivalent axial imperfection component. Good agreement was found between theory and experiment for the range of imperfection amplitudes encountered.

Nomenclature

$A_{ij} = \sum_{k=1}^{r} (\bar{Q}_{ij})_k (h_k - h_{k-1})$

$B_{ij} = \frac{1}{2} \sum_{k=1}^{r} (\bar{Q}_{ij})_k (h_k^2 - h_{k-1}^2)$

$C_j = \frac{1}{L} \int_{-L/2}^{L/2} w(x) e^{-i\omega_j x} dx$

$D_{ij} = \frac{1}{3} \sum_{k=1}^{r} (\bar{Q}_{ij})_k (h_k^3 - h_{k-1}^3)$

$[A^*] = [A^{-1}]$
$[B^*] = -[A^{-1}][B]$
$[C^*] = [B][A^{-1}]$
$[D^*] = [D] - [B][A^{-1}][B]$

E_{11}, E_{22}, G_{12} = orthotropic elastic constants
F = Airy stress function
k = refers to kth lamina
l_x = $L/2m$, axial half-wavelength
$l_{x_{cr}}$ = $\pi(1+\beta^2)^{1/4}(R/\gamma)^{1/2}$
l_{x_j} = imperfection half-wavelength corresponding to the jth Fourier term
L = shell length
m, n = number of axial and circumferential waves, respectively
N_0 = compressive load per unit length
p = $\pi R/2l_x$
Q_{11} = $E_{11}/(1 - \nu_{12}\nu_{21})$
Q_{22} = $E_{22}/(1 - \nu_{12}\nu_{21})$
Q_{12} = $\nu_{21}E_{11}/(1 - \nu_{12}\nu_{21}) = \nu_{12}E_{22}/(1 - \nu_{12}\nu_{21})$
Q_{66} = G_{12}
$\bar{Q}_{11}$ = $Q_{11}C^4 + 2(Q_{12} + 2Q_{66})S^2C^2 + Q_{22}S^4$
$\bar{Q}_{22}$ = $Q_{11}S^4 + 2(Q_{12} + 2Q_{66})S^2C^2 + Q_{22}C^4$
$\bar{Q}_{12}$ = $(Q_{11} + Q_{22} - 4Q_{66})S^2C^2 + Q_{12}(S^4 + C^4)$
$\bar{Q}_{66}$ = $(Q_{11} + Q_{22} - 2Q_{12} - 2Q_{66})S^2C^2 + Q_{66}(S^4 + C^4)$
$\bar{Q}_{16}$ = $(Q_{11} - Q_{12} - 2Q_{66})SC^3 + (Q_{12} - Q_{22} + 2Q_{66})S^3C$
$\bar{Q}_{26}$ = $(Q_{11} - Q_{12} - 2Q_{66})S^3C + (Q_{12} - Q_{22} + 2Q_{66})SC^3$
r = total number of composite laminae
R = shell radius measured to midsurface
S, C = $\sin\theta, \cos\theta$, respectively
t = thickness
$\bar{t}$ = total average thickness of shell wall
x, y = axial and circumferential coordinates, respectively, of reference surface
w = radial displacement
α = $D_{11}^*/(A_{22}^* D_{11}^*)^{1/2}$
β = $B_{21}^*/(A_{22}^* D_{11}^*)^{1/2}$
γ = $1/(A_{22}^* D_{11}^*)^{1/2}$
θ = orientation of fibre axes relative to structural axes
λ = $N_0 R/2\alpha$ nondimensional load parameter
λ_{cr} = nondimensional experimental buckling load for imperfect shell
λ_0 = buckling load corresponding to asymmetric solution for $\mu = 0$
λ^* = λ_{cr}/λ_0
μ = imperfection amplitude
μ_k = $\mu/\bar{t}$
ν_{12}, ν_{21} = major and minor Poisson's ratio of orthotropic material, respectively
ρ = $(2p^2/R\gamma)^{1/2}$ reduced axial wave number
τ = $(2n^2/R\gamma)^{1/2}$ reduced circumferential wave number
ω_j = π/l_{x_j}, spatial frequency
$\bar{\omega}_j$ = $l_{x_{cr}}/l_{x_j}$

$$\nabla_{A^*}{}^4 = A_{22}^* \frac{\partial^4}{\partial x^4} - 2A_{26}^* \frac{\partial^4}{\partial x^3 \partial y} + (2A_{12}^* + A_{66}^*) \frac{\partial^4}{\partial x^2 \partial y^2} - 2A_{16}^* \frac{\partial^4}{\partial x \partial y^3} + A_{11}^* \frac{\partial^4}{\partial y^4}$$

$$\nabla_{D^*}{}^4 = D_{11}^* \frac{\partial^4}{\partial x^4} + 4D_{16}^* \frac{\partial^4}{\partial x^3 \partial y} + 2(D_{12}^* + 2D_{66}^*) \frac{\partial^4}{\partial x^2 \partial y^2} + 4D_{26}^* \frac{\partial^4}{\partial x \partial y^3} + D_{22}^* \frac{\partial^4}{\partial y^4}$$

$$\nabla_{B^*}{}^4 = B_{21}^* \frac{\partial^4}{\partial x^4} + (2B_{26}^* - B_{61}^*) \frac{\partial^4}{\partial x^3 \partial y} + (B_{11}^* + B_{22}^* - 2B_{66}^*) \frac{\partial^4}{\partial x^2 \partial y^2} + (2B_{16}^* - B_{62}^*) \frac{\partial^4}{\partial x \partial y^3} + B_{12}^* \frac{\partial^4}{\partial y^4}$$

Presented as Paper 72-139 at the AIAA 10th Aerospace Sciences Meeting, San Diego, Calif., January 17–19, 1972; submitted March 21, 1972; revision received August 29, 1972. The authors wish to acknowledge the financial assistance of Fleet Manufacturing Ltd. (DIR Contract M-37) and the National Research Council of Canada (Grant 2783). The shell test models were supplied by N. S. Khot of the Air Force Flight Dynamics Laboratory (Structures Division), Wright-Patterson Air Force Base, Ohio.

Index category: Structural Stability Analysis.

* Associate Professor, Institute for Aerospace Studies. Member AIAA.

† Research Engineer; currently Assistant Professor, Faculty of Applied Science and Engineering, Memorial University of Newfoundland, St. John's, Newfoundland, Canada.

Introduction

IN the design of cylindrical shell structures, buckling under compressive loading constitutes one of the primary considerations. Current design manuals[1,2] require that classical buckling

loads be reduced by an empirical "correlation" factor which is based on an accumulation of circular cylinder test data through which a conservative curve was fitted. These arbitrary "knock down" factors, applied to cylinders of any wall construction, result in load reductions which are quite large for $R/t \geq 100$. Thus it is of importance to determine if reliable buckling load predictions can be established using other criteria, particularly for composite shells, in order to benefit from their light-weight construction.

Geometric shape imperfections are generally accepted as the dominant factor in reducing the buckling load of cylindrical shells under axial compression.[3] Both theoretical[4] and experimental[5,6] work have demonstrated that for small‡ imperfection amplitudes, uniform axisymmetric shape imperfections in the shape of the classical axisymmetric buckling mode have the most degrading effect on the buckling load for isotropic cylinders. Furthermore, the decrease in buckling strength associated with circumferential imperfection components is relatively small[7] compared to that for axial distributions.

Similar theoretical studies[8-10] on the effects of shape imperfections on the buckling behavior of laminated anisotropic circular cylinders have also been made. The most recent work[10] considered a uniform axisymmetric imperfection, the results of which form the basis for predicting the buckling loads of the shell models used in this program. From buckling tests performed by other investigators[11-13] on composite cylinders, experimental results were found to lie within 65–85% of the theoretical loads for perfect shells using linear anisotropic theory. In general, the disparity between buckling tests and theoretical predictions for anisotropic shells was comparable with that for isotropic cylinders. Consequently, a program was initiated to investigate the buckling behavior of three-ply, laminated glass-epoxy circular cylinders under axial compression. The major objective was to determine if the buckling strength of well-characterized composite shells containing random distributions of shape imperfections could be accurately estimated based on the maximum value of the rms imperfection amplitude.

Basic Theory

In order to predict the buckling load for laminated anisotropic cylinders under axial compression, consideration of random shape imperfections is necessary for practical shell configurations. Since a general random imperfection analysis is a formidable task, it was decided to investigate the effect of a uniform axisymmetric shape imperfection of the form

$$w_0(x) = -\mu \cos 2px/R \tag{1}$$

which constitutes the most degrading case. The appropriate nonlinear equilibrium and compatibility equations for thin laminated anisotropic circular cylinders, including an initial axisymmetric stress-free radial displacement, are given by[10]

$$\begin{bmatrix} \nabla_{A^*}{}^4 & -\nabla_{B^*}{}^4 \\ \nabla_{B^*}{}^4 & \nabla_{D^*}{}^4 \end{bmatrix} \begin{bmatrix} F \\ w \end{bmatrix} = \begin{bmatrix} \left(\dfrac{\partial^2 w}{\partial x \partial y}\right)^2 - \dfrac{\partial^2 w}{\partial y^2} \times \left(\dfrac{\partial^2 w}{\partial x^2} + \dfrac{\partial^2 w_0}{\partial x^2}\right) + \dfrac{1}{R}\dfrac{\partial^2 w}{\partial x^2} \\ \dfrac{\partial^2 F}{\partial y^2}\left(\dfrac{\partial^2 w}{\partial x^2} + \dfrac{\partial^2 w_0}{\partial x^2}\right) - 2\dfrac{\partial^2 F}{\partial x \partial y}\left(\dfrac{\partial^2 w}{\partial x \partial y}\right) + \dfrac{\partial^2 F}{\partial x^2}\left(\dfrac{\partial^2 w}{\partial y^2} - \dfrac{1}{R}\right) \end{bmatrix} \tag{2}$$

Following the analytic procedure of Koiter described in his "special theory,"[4] approximate solutions to Eqs. (2) were obtained[10] assuming that the shell was free to rotate circumferentially and did not deform into a torsional buckling mode. Linear theory was then used to investigate the stability of the fundamental state by considering a small perturbation from the elementary solution. The linearized governing equations were subsequently solved by a Galerkin procedure to obtain an upper-bound estimate of the critical load. The following eigenvalue equation (derived in Ref. 10) leads to buckling loads (λ_{cr}) for axisymmetric imperfect laminated anisotropic shells

$$A_2\lambda^3 - (A_1 + 2A_2C_1 + A_4)\lambda^2 + (2A_1C_1 + A_2C_1{}^2 + A_4C_1 + A_3)\lambda - (A_1C_1{}^2 + A_3C_1 + A_5) = 0 \tag{3}$$

where the coefficients are defined in Appendix A. The perfect shell classical buckling loads (λ_0) can readily be obtained by setting the imperfection amplitude to zero. Thus,

$$\lambda = (\gamma/4\alpha\rho^2)\{[(a_{11}b_{11}' - a_{22}b_{22})b_{11}' + (a_{11}b_{22} - a_{22}b_{11}')b_{22}]/(a_{11}{}^2 - a_{22}{}^2) + d_{12}\} \tag{4}$$

Because of the large number of coefficients involved, numerical evaluation of Eqs. (3) and (4) was carried out on a digital computer. For the particular case of a three-ply, glass-epoxy composite cylinder with fiber orientations θ, 0, $-\theta$, it was found that drastic buckling load reductions occurred, comparable to isotropic shells, for small values of imperfection amplitude (Fig. 1). From a design viewpoint, it can be seen in Fig. 1 that varying fiber orientation for an initially imperfect shell results in only small changes in imperfection sensitivity. Similar behavior was also found for boron-epoxy and graphite-epoxy cylinders, as shown in Fig. 2, where the lower-bound buckling load curves are compared. In addition, the existence of a critical imperfection wavelength corresponding to a minimum buckling load was established.[10] As $\mu \to 0$, the critical half-wavelength approaches

$$l_{x_{cr}} = \pi(1 + \beta^2)^{1/4}(R/\gamma)^{1/2} \tag{5}$$

which is the classical axisymmetric buckling mode for a perfect shell.

If no coupling exists such that $B_{21}{}^* = 0(\beta = 0)$, then $\rho^2 = \frac{1}{2}$ and $l_{x_{cr}} = \pi(R/\gamma)^{1/2}$.

In order to employ the above analysis to predict the buckling strength of a cylinder containing a random distribution of imperfections, it is necessary to determine an equivalent uniform axisymmetric imperfection amplitude based on the rms imperfection measurements obtained from several generator traces for each test model. From Eq. (1), the rms imperfection amplitude for this distribution is given by

$$\delta_{rms} = \mu/2^{1/2} \tag{6}$$

Thus, it is proposed that Eq. (6) can be used to compute an equivalent imperfection using the largest measured value of δ_{rms} for each cylinder. The justification for this assumption derives from the fact that the uniform axisymmetric imperfection, with a wavelength equal to that of the classical axisymmetric buckling mode, constitutes the most degrading case in terms of load reduction, and the effect of the asymmetric distribution can be taken into account by using the maximum value of δ_{rms}. It is assumed that the asymmetric distribution has no terms that exceed the shell wall thickness in magnitude. For arbitrary values of $2^{1/2}\delta_{rms}/t$, buckling loads can be estimated from Eq. (3). Application of this criterion to a shell with random shape imperfections assumes a generator profile, which can be Fourier analyzed[6] to estimate the imperfection modal components, contains a value at $\omega_j = 1$ which is of the same order of magnitude as (or greater than) all other imperfection components. Large local imperfections which might initiate instability must be considered in terms of their particular wavelength, since averaging over the shell length will lead to incorrect results.

‡ Imperfections of the order of the shell wall thickness.

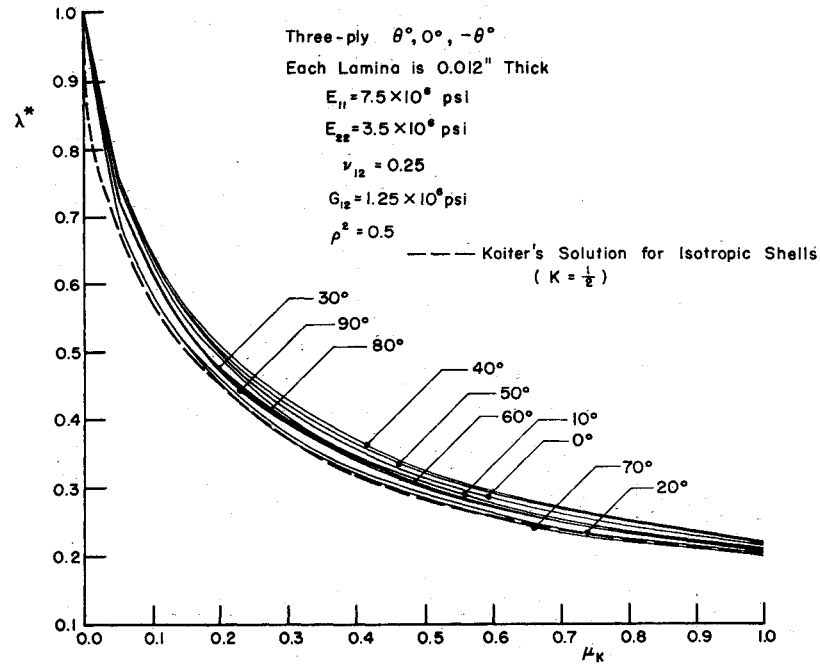

Fig. 1 The effect of imperfection amplitude and fiber orientation on the buckling load of an axisymmetric imperfect composite shell.

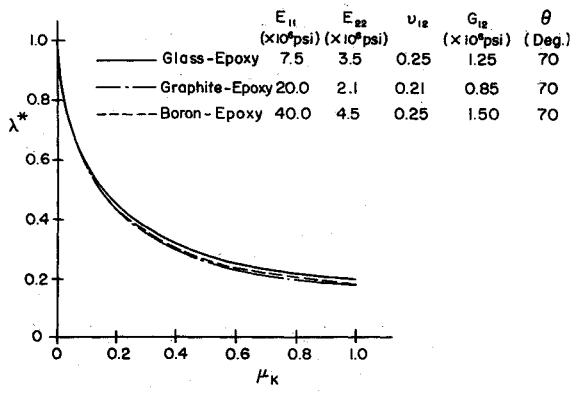

Fig. 2 Lower bound buckling curves for axisymmetric imperfect three-ply ($\theta°$, $0°$, $-\theta°$) laminated circular cylinders.

Experimental Procedure and Results

The experimental phase of the program involved the testing of three-ply, glass-epoxy "Scotchply" (XP250) preimpregnated tape wound cylinders supplied by the Structures Division of the Flight Dynamics Laboratory, Wright-Patterson Air Force Base. Prior to buckling, each shell was subjected to material property characterization tests[13] requiring three loading configurations; internal pressure, torsion and compression. Foil strain gages were bonded in the axial, circumferential and $\pm 45°$ directions at midlength on the outer surface and the resultant stress-strain data was used to compute[13] the orthotropic in-plane material constants. A summary of the geometric and material properties is contained in Tables 1 and 2 for the configurations tested. In some cases, coupons were cut from shells to determine the filament weight content using a resin burn-off test. Rule of mixtures calculations were then made[14] to compare with the orthotropic constants listed in Table 2. Generally, reasonable agreement was obtained.

Each cylinder was mounted in a traversing apparatus having two diametrically opposed, linear, contacting displacement transducers to determine the random distributions of shape imperfections. The output signal, recorded on magnetic tape, was digitized by a sampling voltmeter and this data was fed into a Fourier analysis program. Imperfection amplitudes and an estimated line power spectral density were then computed as a function of spatial frequency (ω_j). Typical results obtained for one of the cylinders are contained in Fig. 3. Average shell wall thickness was also computed from the transducer data. However, since individual laminar thicknesses were required, specimens were polished, etched, and examined under a microscope.

Table 1 Shell geometric properties

Shell no.	θ in.	θ mid.	θ out.	$\bar{t} \times 10^{-3}$, in.	$R/\bar{t}$	L, in	$t_{in.} \times 10^{-3}$, in.	$t_{mid.} \times 10^{-3}$, in.	$t_{out.} \times 10^{-3}$, in.
1a	−70°	70°	0°	27.0	233	12.42	9.0	9.0	9.0
2a	−20°	20°	90°	27.6	228	12.42	9.2	9.2	9.2
3b	90°	90°	90°	28.2	222	10.93	10.2	9.0	9.0
4a	90°	−45°	45°	27.6	226	12.45	9.2	9.2	9.2
4b	90°	−45°	45°	27.3	229	12.45	9.1	9.1	9.1
5b	90°	0°	90°	27.9	224	12.45	9.1	8.7	10.1
6b	45°	0°	−45°	27.2	230	12.42	9.1	9.1	9.0
7b	−45°	45°	90°	26.7	234	12.41	8.9	8.9	8.9
9a	0°	−45°	45°	27.1	231	12.45	9.7	8.7	8.7
9b	0°	−45°	45°	27.0	233	12.40	9.6	8.7	8.7
11a	30°	90°	30°	27.3	229	12.43	9.0	9.3	9.0
11b	30°	90°	30°	27.2	230	12.41	9.0	9.2	9.0
12a	30°	90°	−30°	26.8	234	12.41	8.9	8.9	9.0
12b	30°	90°	−30°	27.6	227	12.41	9.2	9.2	9.2

$R = 6.26$ in.

Table 2 Shell material properties and imperfection amplitudes

Shell no.	$E_{11} \times 10^6$, psi	$E_{22} \times 10^6$, psi	ν_{12}	$G_{12} \times 10^6$, psi	$\delta_{rms} \times 10^{-3}$, in.[b]	μ_k
1a	5.030	2.580	0.345	0.837	0.8932	0.0468
[a]2a	5.420	2.600	0.365	0.687	0.8074	0.0414
3b	5.906	2.921	0.362	0.625	0.9783	0.0491
[a]4a	6.109	2.697	0.317	0.517	0.6622	0.0340
4b	6.109	2.697	0.317	0.517	0.7799	0.0404
5b	5.995	2.600	0.398	0.654	0.5585	0.0283
6b	6.323	1.742	0.435	0.708	0.5333	0.0277
7b	5.424	2.603	0.365	0.687	0.6729	0.0356
9a	6.448	1.823	0.317	0.622	0.5964	0.0311
9b	5.558	1.894	0.413	0.825	0.5940	0.0312
[a]11a	5.420	2.600	0.365	0.687	0.5866	0.0304
[a]11b	5.420	2.600	0.365	0.687	0.4864	0.0252
[a]12a	5.424	2.603	0.365	0.687	0.6866	0.0362
[a]12b	5.420	2.600	0.365	0.687	0.7080	0.0360

$V_{filament} \simeq 70\%$ by wt
50% by vol

[a] Values of material properties assumed.
[b] Largest value of six generator surveys.

All cylinders were fitted with aluminum end plates bonded to the shell wall with a room temperature curing epoxy to provide a clamped edge constraint. In addition, an internal mandrel was positioned inside the shell having a clearance of 0.030 in. in order to minimize postbuckling deformation and thus permit repeat testing. This procedure also allowed adjustments to be made in the alignment of the end platen of the testing machine relative to the cylinder to ensure that uniform buckling occurred. Since it was assumed theoretically that the cylinders were free to rotate during loading, i.e., no induced torques were considered, a thrust bearing was inserted between the top platen and cylinder. It was observed that the buckling loads for cylinders with in-plane anisotropy increased 25% over the values obtained in the torsionally restrained configuration.

Tables 2 and 3 summarize the maximum value of δ_{rms} measured for each shell and compare the predicted imperfect cylinder buckling loads (λ_{imp}) with the experimental values (λ_{cr}). It is quite evident from the results contained in Table 3 that the initial shape imperfections significantly reduced the buckling strength of the cylinders below the "perfect-shell" values (λ_0). The agreement between the predicted response and experiment is consistently good. Although the estimated loads are higher than the experimental values, the differences can probably be attributed to the fact that only six generators were surveyed

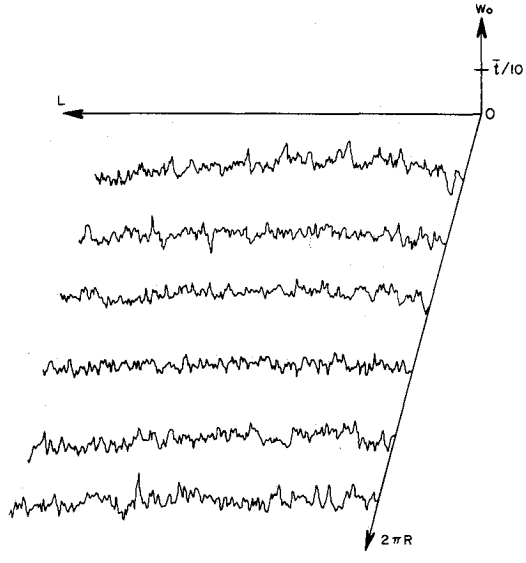

Fig. 3a Median surface random imperfection profiles.

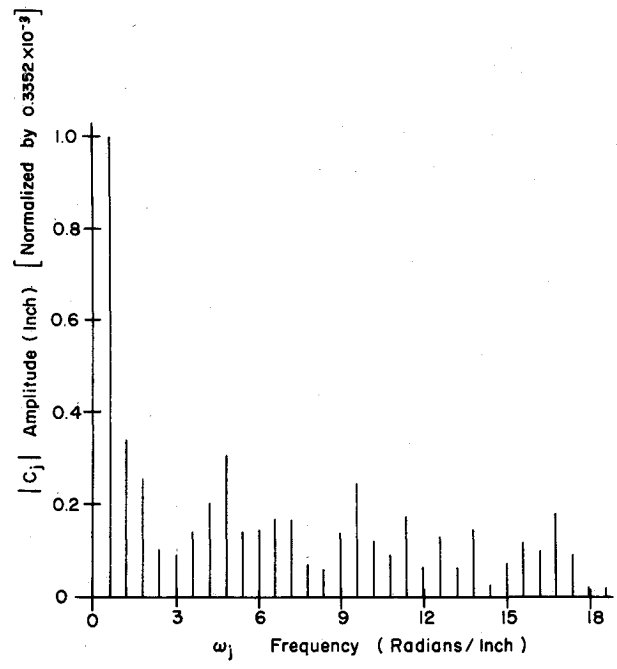

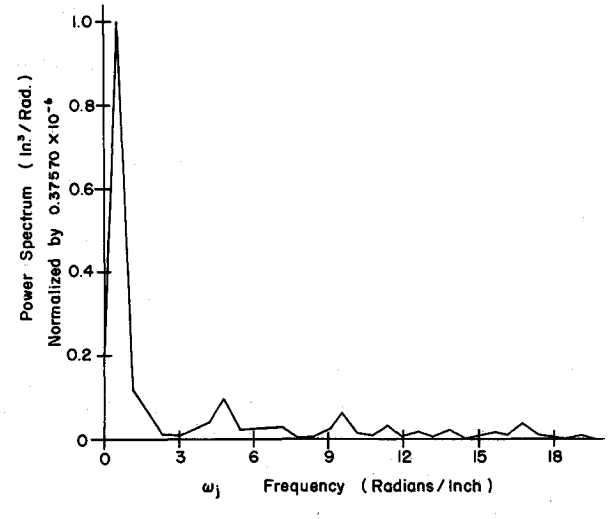

Fig. 3b Estimated frequency and power spectrum of imperfection distribution along a generator.

Table 3 Shell buckling loads

Shell no.	P_{cr} lb.	λ_{cr}	λ_0	$\lambda_{imp.}$	$\lambda^* = \lambda_{cr}/\lambda_0$	$\lambda_{cr}/\lambda_{imp}$
1a	5855	0.598	0.8806	0.6153	0.679	0.972
2a	5525	0.571	0.9266	0.6888	0.616	0.829
3b	5085	0.410	0.6144	0.5015	0.658	0.817
4a	5585	0.655	0.9707	0.7615	0.674	0.860
4b	5075	0.607	0.9707	0.7390	0.625	0.822
5b	5165	0.481	0.6970	0.6029	0.690	0.799
6b	5155	0.765	1.0000	0.8510	0.765	0.899
7b	5595	0.693	0.9224	0.7612	0.751	0.909
9a	5815	0.754	0.9459	0.7815	0.795	0.964
9b	5545	0.686	0.9378	0.7651	0.732	0.896
11a	5865	0.586	0.8136	0.7279	0.720	0.805
11b	6235[a]	0.626	0.8142	0.7486	0.769	0.836
12a	5715	0.641	0.9128	0.7208	0.703	0.889
12b	5655	0.584	0.9107	0.7202	0.641	0.810

[a] Without thrust bearing $P_{cr} = 4945$ lb.

on each cylinder which does not ensure that the maximum δ_{rms} is obtained. Furthermore, imperfection asymmetry, edge constraints and material property variations will also affect the comparison.

Correlation of axisymmetric imperfection theory with test data obtained from cylinders containing random imperfection distributions is based on the assumption that certain frequency components will grow with applied load at such a rate as to initiate buckling. Qualitative evidence of this behavior is shown in Fig. 4 in which a shell generator profile is plotted as a function of applied load. The actual variation of the Fourier coefficients as a function of spatial frequency during loading is plotted in Fig. 5. It can readily be seen that imperfection components other than the critical wavelength become greater in magnitude close to the buckling load because of their initial values. As was demonstrated in Ref. 10, instability is governed both by imperfection amplitude and wavelength. Thus it is quite possible for a noncritical component of sufficient magnitude to control buckling. The design approach used in this analysis, however, considers the maximum rms imperfections to be concentrated at the critical frequency ($\bar{\omega}_j = 1$) in order to estimate a buckling load independent of the imperfection spectrum. This is consistent with the fact that only small variations in the buckling load occur within a relatively large-frequency bandwidth centered at $\bar{\omega}_j = 1$ (Ref. 10).

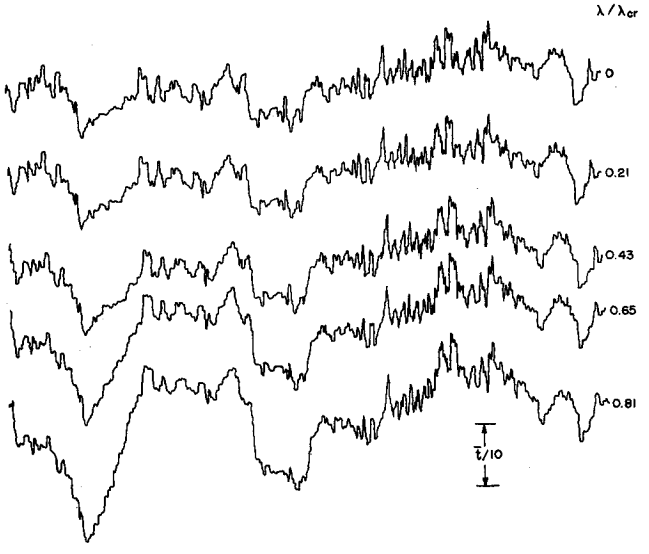

Fig. 4 Imperfection profile for one generator as a function of applied load.

Conclusions

A new design approach has been proposed to provide a conservative estimate of the buckling strength of circular cylindrical laminated composite shells under axial compression. Based on the experimental results obtained from well characterized cylinders, it would appear that the design method yields

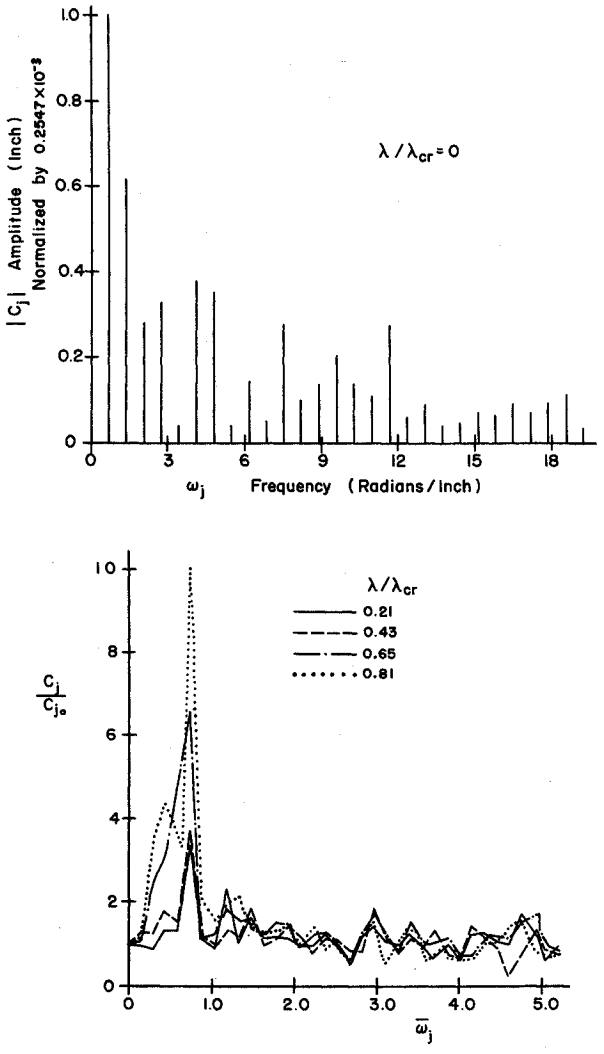

Fig. 5 Variation in Fourier coefficients of imperfection spectrum as a function of spatial frequency and applied load.

accurate estimates of load reductions associated with random imperfections of small mean square amplitude. It is thought that the method should provide a conservative buckling load estimate even for shells that contain general imperfections up to the order of the shell wall thickness.

Appendix A

The coefficients of the eigenvalue equation

$$A_2\lambda^3 - (A_1 + 2A_2C_1 + A_4)\lambda^2 + (2A_1C_1 + A_2{C_1}^2 + A_4C_1 + A_3)\lambda - (A_1{C_1}^2 + A_3C_1 + A_5) = 0 \tag{A1}$$

are

$$\begin{aligned}
A_1 &= d_{12} + \frac{(a_{11}b_{11}' - a_{22}b_{22})b_{11}' + (a_{11}b_{22} - a_{22}b_{11}')b_{22}}{\Delta_1} \\
A_2 &= 4\alpha\rho^2/\gamma \\
A_3 &= 4\mu\rho^2\tau^2(a_{11}b_{11}' - a_{22}b_{22})C_1/\Delta_1 \\
A_4 &= \mu\alpha(1 - 2\rho^2\beta)\tau^2 \\
A_5 &= 4\mu^2\rho^4\tau^4{C_1}^2(a_{11}/\Delta_1 + a_{13}/\Delta_3) \\
C_1 &= \rho^2 + (1 - 2\rho^2\beta)^2/4\rho^2 \\
a_{1i} &= {A_{22}}^*(2i-3)^4\rho^4 + (2{A_{12}}^* + {A_{66}}^*)(2i-3)^2\rho^2\tau^2 + {A_{11}}^*\tau^4 \\
a_{2i} &= 2{A_{26}}^*(2i-3)^3\rho^3\tau + 2{A_{16}}^*(2i-3)\rho\tau^3 \\
b_{1i} &= {B_{21}}^*(2i-3)^4\rho^4 + ({B_{11}}^* + {B_{22}}^* - 2{B_{66}}^*)(2i-3)^2\rho^2\tau^2 + {B_{12}}^*\tau^4 \\
b_{2i} &= ({B_{61}}^* - 2{B_{26}}^*)(2i-3)^3\rho^3\tau + ({B_{62}}^* - 2{B_{16}}^*)(2i-3)\rho\tau^3 \\
b_{1i}' &= (b_{1i} - 2(2i-3)^2\rho^2/\gamma) \\
\Delta_i &= ({a_{1i}}^2 - {a_{2i}}^2) \\
d_{1i} &= {D_{11}}^*(2i-3)^4\rho^4 + (2{D_{12}}^* + 4{D_{66}}^*)(2i-3)^2\rho^2\tau^2 + {D_{22}}^*\tau^4
\end{aligned} \tag{A2}$$

Equations (A2) define the coefficients of Eq. (A1) in terms of the anistropic shell material properties and geometry. The critical buckling load (λ_{cr}) for the axisymmetric imperfect shell corresponds to the smallest positive root λ of Eq. (A1) using τ (the circumferential wave number) as the minimization parameter.

References

[1] Baker, E. H., Cappelli, A. P., Kovalevsky, L., Rish, F. L., and Verette, R. M., "Shell Analysis Manual," NASA CR-912, April 1968.

[2] "Buckling of Thin-Walled Circular Cylinders," *Space Vehicle Design Criteria (Structures)*, NASA SP-8007, Aug. 1968.

[3] Hutchinson, J. W. and Koiter, W. T., "Post-Buckling Theory," *Applied Mechanics Reviews*, Vol. 23, No. 12, Dec. 1970, pp. 1353–1366.

[4] Koiter, W. T., "The Effect of Axisymmetric Imperfections on the Buckling of Cylindrical Shells Under Axial Compression," *Proceedings*, B66, Akademie van Wetenshappen, Konenklijke, Netherlands, 1963, pp. 265–279.

[5] Tennyson, R. C. and Muggeridge, D. B., "Buckling of Axisymmetric Imperfect Circular Cylindrical Shells under Axial Compression," *AIAA Journal*, Vol. 7, No. 11, Nov. 1969, pp. 2127–2131.

[6] Tennyson, R. C., Muggeridge, D. B., and Caswell, R. D. "The Effect of Axisymmetric Imperfection Distributions on the Buckling of Circular Cylindrical Shells under Axial Compression," *Proceedings of AIAA/ASME 11th Structures, Structural Dynamics and Materials Conference*, AIAA, New York, 1970, pp. 146–157; also *AIAA Journal*, Vol. 9, No. 5, May 1971, pp. 924–930.

[7] Tennyson, R. C., Muggeridge, D. B., and Caswell, R. D. "New Design Criteria for Predicting Buckling of Cylindrical Shells under Axial Compression," *Journal of Spacecraft and Rockets*, Vol. 8, No. 10, Oct. 1971, pp. 1062–1067.

[8] Khot, N. S., "On the Influence of Initial Geometric Imperfections on the Buckling and Postbuckling Behavior of Fiber-Reinforced Cylindrical Shells under Uniform Axial Compression," AFFDL-TR-68-136, Oct. 1968, Air Force Flight Dynamics Lab., Wright-Patterson Air Force Base, Ohio.

[9] Khot, N. S. and Venkayya, V. B., "Effect of Fiber Orientation on Initial Postbuckling Behavior and Imperfection Sensitivity of Composite Cylindrical Shells," AFFDL-TR-79-125, Dec. 1970, Air Force Flight Dynamics Lab., Wright-Patterson Air Force Base, Ohio.

[10] Tennyson, R. C., Chan, H. K., and Muggeridge, D. B. "The Effect of Axisymmetric Shape Imperfections on the Buckling of Laminated Anisotropic Circular Cylinders," *Canadian Aeronautics and Space Institute, Transactions of the Institute*, Vol. 4, No. 2, Sept. 1971, pp. 131–139.

[11] Card, M. F., "Experiments to Determine the Strength of Filament-Wound Cylinders Loaded in Axial Compression," TN D3522, Aug. 1966, NASA.

[12] Tasi, J., Feldman, A., and Stang, D. A. "The Buckling Strength of Filament-Wound Cylinders Under Axial Compression," NASA CR-266, 1965.

[13] Holston, A., Jr., Feldman, A., and Stang, D. A., "Stability of Filament-Wound Cylinders Under Loading," AFFDL-TR-67-55, May 1967, Air Force Flight Dynamics Lab., Wright-Patterson Air Force Base, Ohio.

[14] Ashton, J. E., Halpin, J. C., and Petit, P. H., *Primer on Composite Materials: Analysis*, Technomic Publishing Co. Inc., Stamford, Conn. 1969.